Acta Neuropathol (2011) 122:495–510
DOI 10.1007/s00401-011-0867-2

ORIGINAL PAPER

Expression of the progenitor marker NG2/*CSPG4* predicts poor survival and resistance to ionising radiation in glioblastoma

Agnete Svendsen · Joost J. C. Verhoeff · Heike Immervoll · Jan C. Brøgger · Justyna Kmiecik · Aurelie Poli · Inger A. Netland · Lars Prestegarden · Jesús Planagumà · Anja Torsvik · Anneli Bohne Kjersem · Per Ø. Sakariassen · Jan I. Heggdal · Wouter R. Van Furth · Rolf Bjerkvig · Morten Lund-Johansen · Per Ø. Enger · Joerg Felsberg · Nicolaas H. C. Brons · Karl J. Tronstad · Andreas Waha · Martha Chekenya

Received: 30 June 2011 / Revised: 15 August 2011 / Accepted: 15 August 2011 / Published online: 24 August 2011

Abstract Glioblastoma (GBM) is a highly aggressive brain tumour, where patients respond poorly to radiotherapy and exhibit dismal survival outcomes. The mechanisms of radioresistance are not completely understood. However, cancer cells with an immature stem-like phenotype are hypothesised to play a role in radioresistance. Since the progenitor marker neuron-glial-2 (NG2) has been shown to regulate several aspects of GBM progression in experimental systems, we hypothesised that its expression would influence the survival of GBM patients. Quantification of NG2 expression in 74 GBM biopsies from newly diagnosed and untreated patients revealed that 50% express high NG2 levels on tumour cells and associated vessels, being associated with significantly shorter survival. This effect was independent of age at diagnosis, treatment received and hypermethylation of the O^6-methylguanine

Electronic supplementary material The online version of this article (doi:10.1007/s00401-011-0867-2) contains supplementary material, which is available to authorized users.

A. Svendsen · J. Kmiecik · A. Poli · I. A. Netland · J. Planagumà · A. Torsvik · P. Ø. Sakariassen · R. Bjerkvig · P. Ø. Enger · K. J. Tronstad · M. Chekenya
Department of Biomedicine, University of Bergen, 5009 Bergen, Norway

J. J. C. Verhoeff
Laboratory of Experimental Oncology and Radiobiology, Academic Medical Center, University of Amsterdam, Amsterdam, The Netherlands

H. Immervoll
Department of Pathology, Haukeland University Hospital, 5021 Bergen, Norway

J. C. Brøgger
Department of Neurology, Haukeland University Hospital, 5021 Bergen, Norway

A. Poli · R. Bjerkvig · N. H. C. Brons
Centre de Recherche de Public de la Santé, Luxembourg, Haukeland University Hospital, Bergen, Norway

L. Prestegarden
Department of Dermatology, Haukeland University Hospital, 5021 Bergen, Norway

A. B. Kjersem
Det Norske Veritas, Johan Berentsensvei 109-111, 5020 Bergen, Norway

J. I. Heggdal
Department of Oncology and Medical Physics, University of Amsterdam, Amsterdam, The Netherlands

W. R. Van Furth
Department of Neurosurgery, Academic Medical Center, University of Amsterdam, Amsterdam, The Netherlands

M. Lund-Johansen · P. Ø. Enger
Department of Neurosurgery, Haukeland University Hospital, 5021 Bergen, Norway

J. Felsberg
Department of Neuropathology, Heinrich-Heine-University, Düsseldorf, Germany

A. Waha
Department of Neuropathology, University Hospital Bonn, Bonn, Germany

M. Chekenya (✉)
Translational Cancer Research Group, Jonas Lies vei 91, 5009 Bergen, Norway
e-mail: martha.chekenya@biomed.uib.no

methyltransferase (*MGMT*) DNA repair gene promoter. NG2 was frequently co-expressed with nestin and vimentin but rarely with CD133 and the NG2 positive tumour cells harboured genetic aberrations typical for GBM. 2D proteomics of 11 randomly selected biopsies revealed upregulation of an antioxidant, peroxiredoxin-1 (PRDX-1), in the shortest surviving patients. Expression of PRDX-1 was associated with significantly reduced products of oxidative stress. Furthermore, NG2 expressing GBM cells showed resistance to ionising radiation (IR), rapidly recognised DNA damage and effectuated cell cycle checkpoint signalling. PRDX-1 knockdown transiently slowed tumour growth rates and sensitised them to IR in vivo. Our data establish NG2 as an important prognostic factor for GBM patient survival, by mediating resistance to radiotherapy through induction of ROS scavenging enzymes and preferential DNA damage signalling.

Keywords Radiation resistance · NG2 · CD133, DNA damage · Peroxiredoxin-1 · Glioblastoma

Introduction

Glioblastoma (GBM) is the most common and malignant primary brain tumour in adults [34]. Although combined radiation and chemotherapy is currently the most effective treatment modality, the patients have a median survival of only 14.6 months [49], due to the tumour's intrinsic resistance to radio- and chemotherapy. Molecular markers that effectively predict response to therapy and survival outcomes are limited. Young age at diagnosis and promoter methylation of the DNA repair gene O^6-methylguanine methyltransferase (*MGMT*) are established predictors of favourable response to radiotherapy and chemotherapy [18, 34]. Reactive oxygen species (ROS) are produced in response to ionising radiation (IR), and mediate its mutagenic and cytotoxic effects. Elevated ROS, in excess of antioxidant enzyme expression, damages DNA, lipids and proteins, ultimately causing tumour cell death [41]. Peroxiredoxins (PRDX) are a large, highly conserved thioredoxin-specific antioxidant family classified by the presence of one or two cysteine residues (1-Cys) and (2-Cys), respectively [40]. PRDX-1 is a major 2-Cys family member whose antioxidant activity modulates responses to IR.

The neural progenitor marker Neuron Glia-2 (NG2), is a 300 kDa transmembrane chondroitin sulphate proteoglycan encoded by the *cspg4* gene on chromosome 15 [31]. The human homologue is the melanoma proteoglycan (MPG) and is aberrantly expressed by several tumour types [2, 8, 25, 28, 43, 44] where it correlates with poor clinical outcome [4, 45]. We have previously demonstrated that NG2 promoted GBM multi-drug chemoresistance mediated by augmented integrin activated PI3K/AKT survival signalling. [10]. We showed also that NG2 promotes tumour growth and angiogenesis in animal models [9, 51]. Given its multifunctional role in GBM biology, we hypothesised that increased proportions of NG2 expressing cells in a GBM may have an impact on patient survival outcomes. Furthermore, some studies have linked therapy resistance to another subpopulation of GBM cells characterised by expression of the neural stem cell marker, CD133/prominin [1]. We therefore investigated the expression patterns of CD133, nestin and vimentin expressing neural stem/progenitor cells and asked whether the NG2 positive tumour cells co-expressed these molecular markers. We demonstrate herein that high NG2 expression on tumour cells and angiogenic vasculature in GBM is associated with shorter survival, independent of patients' age, treatment, and *MGMT* promoter hypermethylation status. NG2 expressing GBM cells harbour genetic aberrations that are typical for the disease, co-express nestin and vimentin but are rarely CD133 positive. At a mechanistic level, we demonstrate that NG2 positive GBM cells with increased PRDX-1 activity show resistance to radiotherapy by rapidly inducing a DNA damage signalling response. Moreover, this response could be counteracted by NG2 and PRDX-1 knockdown in the NG2 expressing cells but not in control NG2 negative cells. Our data establish NG2 as a prognostic factor for poor survival and resistance to IR in GBM and as such may be an amenable therapeutic target. Our findings further contribute to a body of evidence demonstrating that aggressive growth and therapy resistance may not be restricted to a discrete population of tumour cells. Cellular and molecular heterogeneity in GBMs drive these biological features through multiple mechanisms.

Materials and methods

Cell lines and shRNA transduction

The NG2 negative GBM cell line U251N (U251, American Type Culture Collection, Rockville, MA, USA; ATCC) was transfected with NG2 cDNA to produce the U251-NG2 cell line as previously described [9]. HF66 (Ford Cancer Center, Detroit, MI, USA) GBM cell line that endogenously expressed NG2 was propagated as previously described [9]. Due to increasing reports of misidentified cell lines, we verified the identities of all our cell lines by STR analysis, and confirmed these to be bonafide (data not shown).

Retroviral PRDX-1 and irrelevant GFP control shRNA constructs were purchased from Origene (Rockville, MD), and used to generate the stable U251-NG2 shPRDX-1 and U251-NG2-shCTRL cell lines as well control U251

shPRDX-1 and U251 shCTRL cell lines. Stable cell lines were generated by puromycin selection, according to the manufacturer's protocols. To validate our findings in another cell line, the high endogenous NG2 expressing HF66 cells were transduced with lentiviral particles harbouring shRNAs targeting the *cspg4* gene or control scrambled shRNAs according to the manufacturer's protocol (Santa Cruz Biotechnology Inc, Santa Cruz, CA, USA). Briefly, cells were infected at a MOI of 1–2 in the presence of 10 μg/ml Polybrene® (Sigma Aldrich, St. Louis, MO, USA). Stable clones expressing the shRNA constructs were established by 2 μg/ml puromycin selection, and immunoblotting analyses validated knockdowns.

Patient samples

Ninety-six human GBM biopsies were obtained during surgical resections performed at the Haukeland University Hospital, Norway, between 1998 and 2008, and the University Hospital in Düsseldorf, Germany, from 1988 to 2004. In an additional study of GBM stem cell phenotyping, seven GBM biopsies from surgical resections performed in 2010 at Haukeland University Hospital were included. The patients gave their written informed consent and the study was approved by the respective ethical boards in Norway and Germany. Parts of the tumour were snap frozen while other parts were formalin fixed and paraffin embedded (FFPE). H&E-stained sections were prepared to define representative tumour regions as previously described [17] and GBM diagnosis was confirmed according to the World Health Organization (WHO) classification [27] by pathologists (H.I and J.F). Eligibility criteria included availability of follow-up data, less than 50% necrosis in the sample, and only biopsies obtained at primary diagnosis were included. Clinical information was obtained by reviewing the medical records, and death certificates/registers. Patients were followed-up from the date of operation until death or May 2009. At this point only one patient with a NG2 negative tumour was alive. All patients were treated by surgery, radiotherapy and/or chemotherapy and survival determined as the time elapsed from the date of surgery to the date of death.

Immunohistochemistry

FFPE tissue was subjected to immunohistochemistry using the avidin–biotin-peroxidase complex method according to the manufacturer's protocol (Vectastain, Vector laboratories, Burlingame, CA, USA). NG2 staining was performed as previously described [10]. The expression was graded blindly by two independent investigators including a pathologist (H.I) as negative (0); slight (+); moderate (++) or high (+++) on tumour cells, or on vessels based on overall staining intensity and area fraction of positive cells (Table 2). However, due to small groups, 0/+ and ++/+++ were combined (Table 3).

Morphometric quantification of NG2 expression in patient GBM biopsy material

NG2 expression was also quantified using the NIS-Elements™ BR 3.1 software (Nikon Corporation, Tokyo, Japan), 200× magnification (Supplementary Figure ESM 1). The threshold for pixel intensity was determined on the basis of four brain tumour sections stained for NG2, using a Nikon Eclipse 600 microscope (Nikon). This threshold was stored and subsequently applied with identical microscope settings for scoring of all tumour sections, including negative controls stained for MOC31 antibody (Santa Cruz Biotechnology Inc.). Immunopositive elements (pixels above threshold) were measured and expressed as area fraction of the visual field for each tumour section. The NG2 low GBM biopsies had an immunopositive fraction of 5% or less, compared to NG2 high biopsies that had correspondingly 15% or more. The difference in immunopositive fraction was statistically significant (T test, $p = 0.0027$).

Array comparative genomic hybridization

Comparative genomic hybridization was used to determine the gene copy number in high and low NG2 expressing GBMs ($n = 5$), using whole-genome arrays of 2,400 chromosomally mapped BAC clones (Hum.Array1.14) as previously described [47].

Simultaneous immunohistochemistry and in situ hybridization

FFPE patient GBM biopsies were incubated at 58°C o/n, de-paraffinised and rehydrated using the standard procedures. Antigen retrieval was performed in target retrieval solution, pH 9 (DAKO Cytomation, Glostrup, Denmark). The slides were dehydrated and washed in 2× SSC (150 mM NaCl, 15 mM Sodium Citrate, pH7), and denatured in the presence of 10 μl Vysis LSI EGFR Spectrum Orange/CEP7 Spectrum Green probe (Abbott Molecular, Abbott Park, IL, USA) at 75°C for 5 min. The slides were hybridized at 37°C for 36 h in a humidified hybridisation chamber, followed by incubation with anti-NG2 (WB Stallcup, Burnham Institute) o/n at 4°C and AlexaFluor 647-labelled 2°Ab (Invitrogen, Carlsbad, CA, USA). The slides were mounted with DAPI Vectashield, (Vector Labs, Burlingame, CA, USA) and analysed on a Zeiss LSM 510Meta Confocal microscope (Carl Zeiss MicroImaging, Thornwood, NY, USA).

Bisulfite treatment and *MGMT* methylation analysis

For the analysis of *MGMT* promoter methylation, DNA was extracted from snap-frozen tumour tissue using proteinase K digestion and phenol/chloroform extraction whereas for FFPE samples, the QIAamp DNA mini kit (Qiagen, Hilden, Germany) was used. Bisulfite conversion was conducted as previously described [30]. Each tumour and control sample (bisulfite treated DNA from normal brain as negative control, and *Sss*I treated genomic DNA as positive control) was analysed using the same bisulfite preparation as template.

2D electrophoresis

The first dimension of separation was carried out on IPGphore (Amersham Biosciences, Uppsala, Sweden) at 20°C. The protein concentration was adjusted to 600 µg in a sample buffer consisting of 7 M urea, 2 M thiourea, 4% CHAPS, 100 mM DTT, and 1% v/v pharmalyte (Amersham Biosciences) p*I* 3-10, and applied to 18-cm (pH 3–10) linear immobilized pH gradient (IPG) Immobiline DryStrip (Amersham Biosciences) by in-sample rehydration. The strips were applied onto 13.75% v/v acrylamide/*N*,*N*′-methylenebisacrylamide gels (Bio-Rad, Hempstead, UK). The gels were stained with SYPRO Ruby (Bio-Rad) according to the manufacturer's protocol, scanned on the Typhoon laser scanner (Amersham GE Healthcare, Fairfield, CT, USA) and spot analysis was performed on PDQuest software version 8.0 (Bio-Rad).

Protein digestion and mass spectrometry analysis

Differentially expressed protein spots digested in porcine trypsin (Promega, Madison, WI, USA) and the peptides mixed with a-cyano-4-hydroxycinnamic acid (CHCA) (Bruker Daltonics, Bremen, Germany). Mass spectra were generated on an Ultraflex MS/MS (Bruker Daltonics). Data analysis was performed using MASCOT 2.0 software (Matrix science, Boston, MA), the Swiss-Prot and NCB database search. Protein identification was based on peptide mass fingerprinting, percent coverage, Mowse score, number of peptide matches, peak intensity, and match of p*I* and molecular weight with the location of the protein on the 2D gel [42].

Flow cytometric analysis of GBM stem cell phenotype

Seven GBM biopsies from newly diagnosed, untreated patients were dissociated into single cell suspensions with papain at 37°C using the Neuronal Dissociation Kit (Miltenyi Biotec, Bergisch-Gladbach, Germany) according to the manufacturer's protocol. GBM biopsies were stained with the following purified mouse and rat anti-human monoclonal antibodies (mAb): anti-CD45-V450, HI30 (BD Biosciences, Erembodegem, Belgium); anti-Vimentin-FITC, V9 (eBioscience, Vienna, Austria); anti-NG2, 9.2.27 (Santa Cruz Biotechnology Inc.); anti-Nestin-PerCP-Cy5.5, 25/Nestin (BD Bioscience); anti-CD31-PE-Cy7, WM59, (Biolegend, San Diego, CA, USA); anti-CD133/1-APC, AC133 (Miltenyi Biotec, Bergisch Gladbach, Germany). Appropriate isotype controls (ImmunoTools, Friesoythe, Germany) were used in all experiments to determine the level of background staining. The NCH421k GBM cells that are enriched for CD133 [6] were used as positive controls (courtesy of Dr Herold-Mende, Dept Neurosurgery, University of Heidelberg). The anti-NG2 mAb was coupled with Zenon R-PE mouse IgG2a labelling kit, following the supplier's recommendations (Invitrogen, Paisley, UK). Dead cells were excluded by LIVE/DEAD fixable near-infra red dead cells staining (Invitrogen). After 30-min incubation at 4°C, the GBM cell suspensions were washed twice in ice-cold phosphate-buffered saline (PBS, Invitrogen) supplemented with 0.5% BSA and then incubated for an additional 15 min at 4°C and in the dark with Cytofix/Cytoperm solution (BD Biosciences) in order to permeabilise the cells. The intracellular staining using anti-Vimentin and anti-Nestin was performed for 30 min at 4°C in PermWash solution (BD Biosciences). After two washes in PermWash solution, cells were suspended in PBS supplemented with 0.5% BSA and stained with Hoechst solution at 0.1 µg/ml in order to discriminate nuclear cells from debris. The samples were run on a FACSAria™ flow cytometer and analysed with FACSDiva™ software (BD Biosciences). Diagrams were then created using FlowJo flow software version 7.2.5 (Tree Star Inc, Ashland, OR, USA).

Lipid peroxidation assay

The level of thiobarbituric reactive substances (TBARS) was assessed in butanol-extracts of tissue homogenates (10% w/v prepared from frozen samples), according to the manufacturer's protocol (Northwest Life Science Specialties, LCC, Vancouver). The 3rd-derivative absorbance spectra (400–700 nm) were obtained, and malondialdehyde levels were calculated based on the peak value at 510 nm.

Viability and clonogenic assays

Prior to irradiation cells in exponential growth were seeded in conditioned medium in 6-well plates at a density of 300 cells/well. Colonies were stained in 6% glutaraldehyde/0.5% Crystal violet and counted 11 days post-irradiation. Surviving fractions were calculated as previously described [16]. The 3-(4,5dimethylthiazol-2-yl)-5-(3-

carboxymethoxyphenyl)-2-(4-sulfophenyl)-2H-tetrazolium salt (MTS) assay was used in viability assays after 120 h as described by the manufacturer (CellTiter96 Aqueous One Solution Cell Proliferation Assay, Promega, Madison, WI, USA). Cells in exponential growth phase were seeded at 5,000 cells/ml in 96-well plates after exposure to ionising radiation from 2, 5 10, and 20 Gy.

Flow cytometric assessment of cell cycle kinetics

G1-phase checkpoint was analysed by simultaneous measurement of DNA content and bromo-deoxy uridine (BrdU) uptake. After 5 Gy irradiation, the cells were incubated at 37°C for 2 h and pulse-labelled with 10 μM BrdU (BD Pharmingen, San Jose, CA, USA) for 20 min. The cells were fixed and propagated for staining with FITC-labelled anti-BrdU antibody, according to the manufacturers protocol (BD Pharmingen). 7-AAD counterstain was used to visualise DNA content. For G2 checkpoint analyses, irradiated cells were incubated at 37°C for 16 h, harvested and fixed in 3.7% formaldehyde. Cells were immunostained for phosphorylated Histone H3 Ser10 (Cell Signalling, Boston, MA, USA) and nuclei counterstained with propidium iodide according to the manufacturer's protocol. Flow cytometry was performed on Accuri C6, and bivariate data analysed by FlowJo software (Tree Star Inc.).

Western blotting

Immunoblotting was performed using NuPage gel systems (Invitrogen), lysates were prepared according to the Kinexus protocol (http://www.kinexus.ca) 15 min post-irradiation. Western blotting for PRDX-1 from mice brains was performed on homogenates from the right (site of tumour implantation) and the left hemisphere (normal brain). The band intensity of PRDX-1 in the tumour was quantified using densitometry, and expressed as fold change from the normal brain, normalised for β-actin. Antibodies used: Phospho-ATM (Ser1981); ATM (D2E2); Phospho-Chk2 (Thr68); Chk2; phospho-ASK (Thr845); ASK; pH2AX (Cell Signalling), PRDX-1 (Abcam, Cambridge, UK); NG2 (WB Stallcup, Burnham Institute); β-actin (Abcam).

Surgical procedures and ionising radiation

In vitro ionising radiation was given as 2, 5, 10 and 20 Gy doses at a rate of 3.1 Gy/min with a Clinac 600C/D linear accelerator irradiator (Varian Medical Systems Inc., Palo Alto, CA, USA). Fifty-four, 4 to 6-week old athymic Nude-*nu* female mice (Harlan, Horst, The Netherlands) were xenografted intracranially with 5×10^5/3 μl PBS U251, U251-NG2 ctrl shRNA or U251-NG2 PRDX-1shRNA cells. Three weeks prior to the cell implantation, a hollow guide-screw was implanted right fronto-lateral in the skull, through which cell suspensions were injected 2 mm below the screw, see Fig. 6a. At the onset of irradiation, starting 14 days post-implantation, a 0.2 mCi iodine-125 (^{125}I) seed (IBt, Seneffe, Belgium) was inserted though the hollow screw as described previously [50]. After 26 days mice were sacrificed to enable tumour analysis.

Statistical analyses

Patient survival was analysed using the Kaplan–Meier and the log rank test with Stata 11.0 software (StataCorp LP, College Station, TX, USA). Cox regression was used to adjust for age as a categorical variable, below 60, between 60 and 70, and 75 years and above. A probability ≤ 0.05 was considered significant. The two-tailed Student's *t* test, one way- or two way-analysis of variance (ANOVA) and Chi-square analyses were performed using Graphpad Prism 5.0 (Graphpad Software, La Jolla, CA, USA).

Results

High NG2 expression associates with poorer survival in GBM patients

To determine the relevance of aberrant NG2 expression in GBM progression, we quantified expression in 96 unassigned patient GBM biopsies and correlated the expression with survival outcomes. The patient sample group had a median survival of 12 months (Supplementary Figure ESM 1a), mean and median age of 59.5 and 63.2 years, respectively. The mean and median follow-up was 12.2 and 11.4 months, respectively. Complete clinical data was available for 74 patients. There was no significant difference in the treatment received in the high versus low NG2 expressing patients (Chi-square 2.42, $p = 0.49$). 92.4% of all the patients received temozolomide in combination with radiation and 9.5% received procarbazine and vincristine (PCV) in addition. 13% of the patients that received conventional fractionated whole brain radiation also received gamma knife radiosurgery. Histopathological examination revealed that NG2 was predominantly expressed on the surface of tumour cells (Fig. 1a[2, 6]), as well as on the highly pleomorphic tumour cells in different patients (Fig. 1a[3, 7]). NG2 was also expressed on the tumour vasculature, in particular, on the glomeruloid-like microvascular proliferations in the vicinity of pseudopalisading necroses (Fig. 1a[4, 8]) but rarely on normal appearing capillary vessels. 36% ($n = 27$) of the 74 GBM cases expressing high NG2 levels on the tumour cells also highly expressed it on the tumour vasculature. 15% ($n = 11$) of cases expressed high NG2 levels only on the tumour cells, while 19% ($n = 15$) highly expressed it only on

the vasculature. 28% ($n = 21$) expressed little or undetectable levels of NG2 on the tumour cells or vasculature. Array comparative genomic hybridisation (CGH) performed on a subset of the GBM biopsies confirmed multiple genetic aberrations characteristic of GBM in both the high and low NG2 expressing GBM patient samples (Fig. 1b; Table 1) [29]. To prove that the highly pleomorphic NG2 positive tumour cells were indeed neoplastic, we hybridised the sections with a probe for epidermal growth factor receptor (EGFR), one of the most frequently amplified genes in GBM [29] and simultaneously stained them for NG2. The NG2 positive cells were shown to harbour gross chromosomal alterations, including EGFR and centrosome 7 amplification (Fig. 1c). Kaplan–Meier survival analysis demonstrated a significantly shorter median survival of 8 months for the NG2 high ($n = 38$), compared to the NG2 low ($n = 36$) expressing patients, that had a median survival of 12.5 months. The difference in survival was statistically significant whether NG2 was highly expressed on tumour cells or the associated vasculature (Log Rank test$_{5.196}$, $df = 1$, $p = 0.03$ and $p = 0.02$), respectively, Fig. 1d; Tables 2, 3). The patients that highly expressed NG2 only on the tumour cells or vasculature had median survival of 11 and 12 months, respectively, and there was no significantly increased mortality in these patients when compared to the NG2 low tumour/low vessel group (ANOVA, $p = 0.3$ and $p = 0.2$, respectively) that had a median survival of 13 months. However, the Cox regression hazard ratios were 1.52 and 1.60 increased risk of death in the patients that highly expressed NG2 only on the tumour cells or only on the vasculature, respectively, compared to the low NG2 expressors. This lack of statistical significance may be due to the small

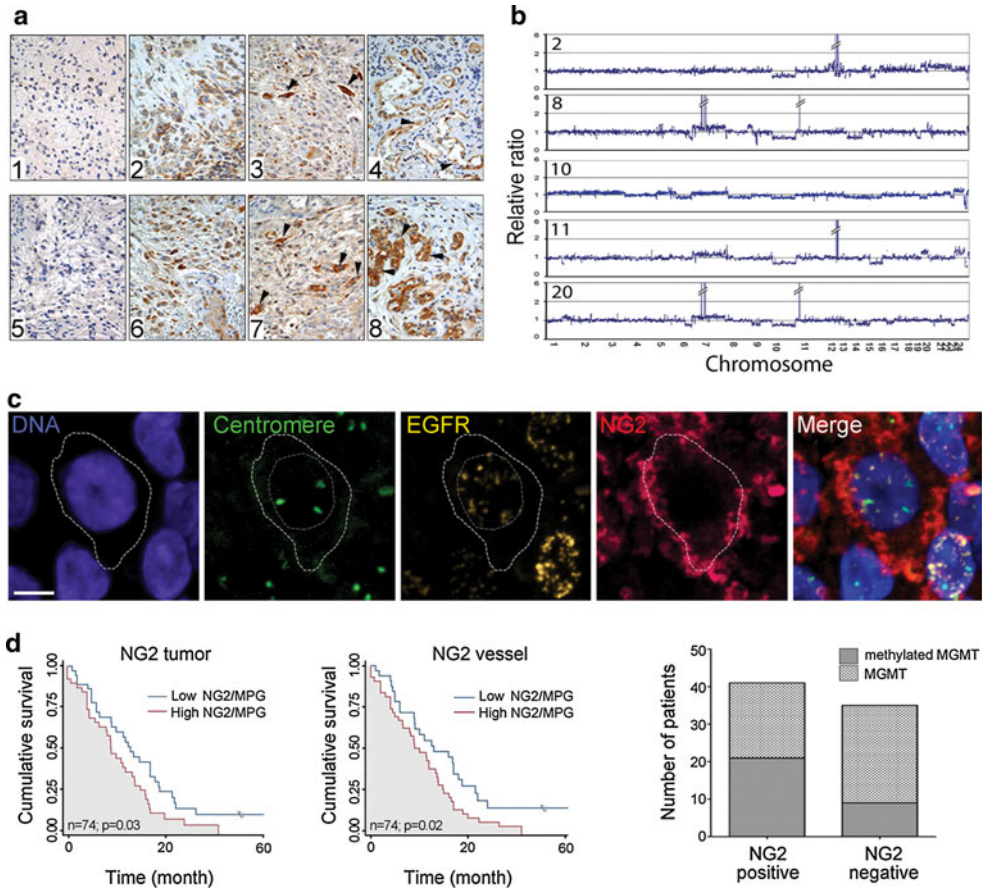

Fig. 1 High NG2 expression is prognostic for poor survival independent of *MGMT* promoter methylation. **a** Immunohistochemistry staining for NG2 in representative GBM examples of NG2 negative tumours (*1* and *5*); NG2 positivity mostly on tumour cells (*2* and *6*), on the most pleomorphic tumour cells (*arrowheads* in *3* and *7*), and on vessels and microvascular proliferations (*arrowheads* in *4* and *8*). **b** Array CGH demonstrating genetic aberrations indicated by loss of chromosomes 6, 9, 10, 13 and 14, as well as gains on chromosomes 7, 12, 15 and 21, consistent with GBM diagnosis in patient material of NG2-low (*2* and *10*) and NG2-high (*8*, *11*, *20*) tumours. **c** Simultaneous fluorescent immunostaining of NG2 (*red*) and fluorescent in situ hybridisation for EGFR (*orange*) and centromere 7 (*green*) amplifications. Nuclear counterstain (*blue*) by DAPI. **d** *Left* Kaplan–Meier survival curves for high versus low NG2 expressors on tumour cells, *Middle* Kaplan–Meier survival curves for high versus low NG2 expressors on vasculature, *Right* Proportion of patient GBMs exhibiting *MGMT* promoter hypermethylation versus unmethylated promoter in the groups of NG2 positive and NG2 negative tumours

Table 1 Chromosomal gains and losses involving genes important for GBM progression in newly diagnosed and untreated patients

Patient	Chromosomal losses	Genes	Chromosomal gains	Genes
2	10	PTEN	12q, 15p, 21	MDM2, Gli1
8	9p, 10, 13, 18q	p16, PTEN	7 (gain and amp)	EGFR
10	10	PTEN	7 (gain)	EGFR
11	10	PTEN	7 (gain), 12 (amp)	EGFR, MDM2, Gli1
20	6q, 9p, 10, 14	p16, PTEN	7 (gain and amp)	EGFR

Summary of genetic alterations detected by array CGH involving genes of known relevance to GBM progression

Table 2 NG2 expression on tumour and vessel

NG2 vessel	NG2 tumour				
	0	+	++	+++	Total
0	3	7	1	3	14
+	2	9	1	6	18
++	0	0	1	0	1
+++	1	14	0	26	41
Total	6	30	3	35	74

Immunohistochemical staining was semi-quantitatively determined as 0/no expression, +/low expression, ++/moderate expression or +++/high expression. The quantification was performed for both tumour and vessel expression

patient numbers in these groups. In contrast, the patients that highly expressed NG2 on both tumour cells and microvascular proliferations had a significantly shorter median survival of 8.2 months compared to 13 months in the patients expressing low NG2 levels on both tumour cells and microvascular proliferations, $p = 0.005$, (hazard ratio 2.55). Morphometric quantification of NG2 levels on both tumour cells and angiogenic vessels revealed significant differences in NG2 levels in the high and low expressors (Supplementary Figure ESM 1b, *t* test, $p = 0.0027$) confirming the pathologists grading, Supplementary Figure ESM 1d. Although some tumours were completely NG2 negative, the majority had varying levels of expression from reduced intensity and immunopositive area fraction to highly intense immunopositivity and large area fraction. Since age at diagnosis is a major prognostic factor, we adjusted for this variable. The hazard ratio before adjusting for age was $HR_{1.313}$ ($p = 0.03$). However, after adjusting for age, (<60, 60–70, ≥75 years) the significance level of NG2 expression on survival was even stronger, $HR_{1.36}$ ($p = 0.0177$). The effect of age on survival had a hazard ratio of 2.09 for ages 60–70, and 2.81 in the group aged ≥75 years. In addition, 51% of the NG2 positive tumours contained methylated *MGMT* promoter, compared to 26% of the NG2 negative tumours (Fishers exact test, $p = 0.03$; Fig. 1d). Taken together, the association of NG2 expression with poorer survival was independent of clinical treatment, age and *MGMT* promoter methylation status.

Table 3 NG2 expression on tumour and vessel combining groups 0/+ and ++/+++

NG2 vessel	NG2 tumour		
	0/+	++/+++	Total
0/+	21	11	32
++/+++	15	27	42
Total	36	38	74

Due to small group numbers, 0/+ and ++/+++ categories were grouped into NG2 low and high expressors, respectively. The survival outcomes were calculated as time elapsed from date of operation until date of death

NG2 expressing cells are phenotypically distinct from CD133 positive tumour cells

Since multiple progenitor cells express NG2 during normal tissue development, we aimed to establish whether NG2 was co-expressed with other markers of immature cells in GBM tumours. Using flow cytometry, we investigated tumour cells from seven dissociated surgical specimens for expression of NG2, nestin, vimentin and CD133. Viable cells were selected for analysis by excluding dead cells by live/dead staining and excluding debris by including only Hoechst positive nucleated cells (Fig. 2a). Furthermore, the cells were gated on CD45- and CD31-populations to exclude immune and endothelial cells, respectively, and ensure subsequent analysis of tumour cells (Fig. 2b). We asked what percentage of tumour cells were NG2, nestin and vimentin positive and whether these subpopulations were coincident with CD133 positive cells. A large proportion of the GBM cells were NG2 and nestin double positive, 50.2 ± 8.4%, $n = 7$ (Fig. 2c). The majority of these cells were also positive for vimentin, 94.5 ± 2.4%, $n = 7$ (Table 4) and negative for CD133, 1.75 ± 1.2%, $n = 7$ (Fig. 2d). NG2 was variably expressed in these GBMs (Fig. 2e; Table 4). These results are consistent with qualitative immunohistochemical analyses presented in Fig. 1. A majority of NG2 positive cells co-expressed the intermediate filaments nestin and vimentin, confirming their immature phenotype. NG2/nestin positive cells rarely co-expressed CD133 ($p = 0.0021$, Mann–Whitney *U* paired, two-tailed *t* test, Fig. 2; Table 4). These studies confirmed that NG2 positive tumour cells represent an immature, mesenchymal differentiation phenotype and the majority of these are distinct from CD133 positive populations.

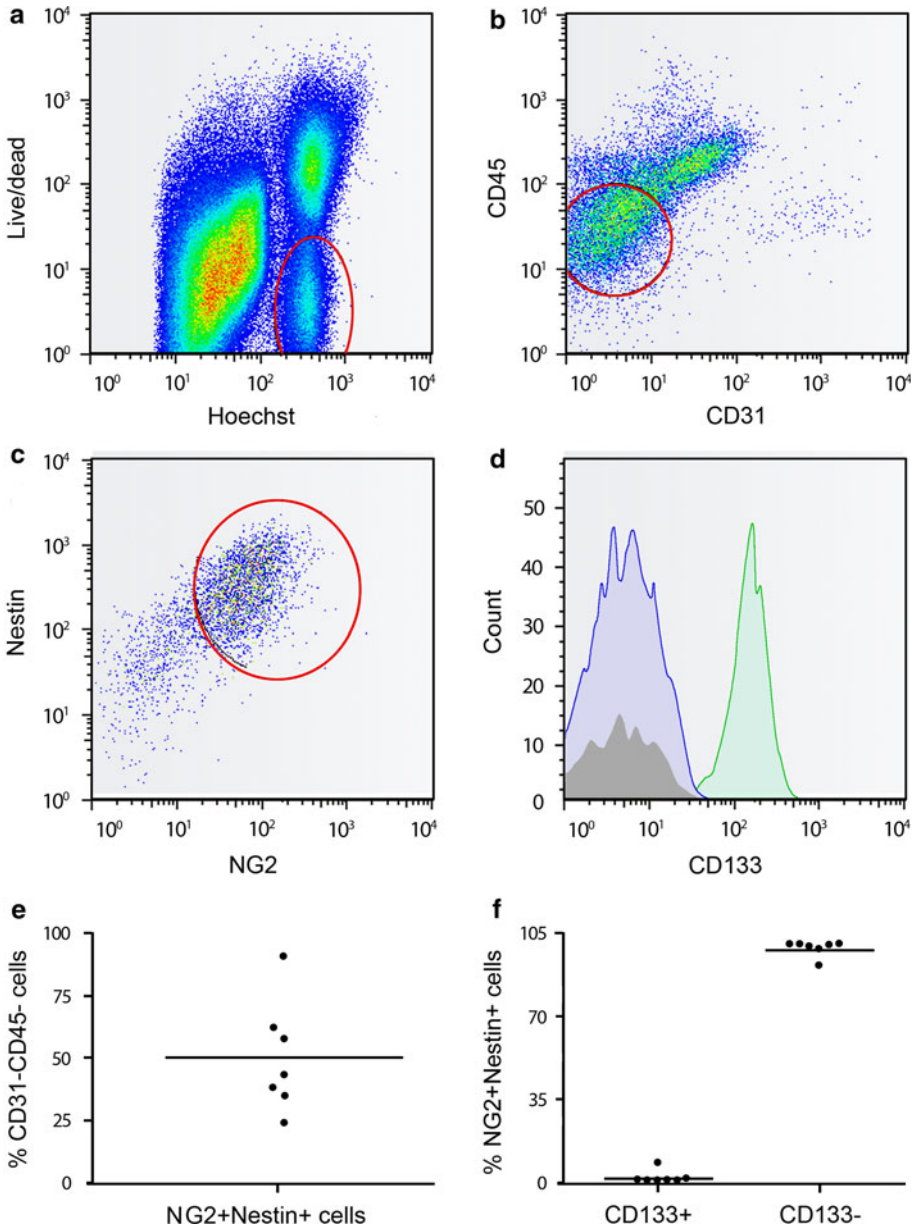

Fig. 2 Expression of CD133 on the NG2+ subpopulation of tumour cells in patient biopsies. **a** Representative gating strategy from patient 2,010-046 showing viable cells gated on Live/dead negative and Hoechst positive nucleated cells. **b** Tumour cells were discriminated from immune and endothelial cells by excluding CD45+ and CD31+ cells, respectively. **c** % tumour cells double positive for NG2 and Nestin. **d** Representative histogram showing CD133 expression by the NG2+/Nestin+ cells (*blue*), CD133 isotype control (*dark shaded region*), NCH421k GBM cells enriched for CD133 used as positive control (*green*). **e** % tumour cells positive for NG2/nestin levels in the CD31–CD45-gated cells. **f** The NG2/nestin expressing tumour cells have low CD133 expression, $p = 0.0021$, Mann–Whitney *U* paired *t* test

PRDX-1 is highly expressed in GBMs from the patients with shortest survival

Next, we aimed to identify protein signatures associated with the survival outcomes using proteomic analyses. PDQuest statistical software identified 15 spots that significantly differentiated the high from the low NG2 expressing biopsies, $p < 0.05$. One of the spots was identified in all the NG2 high patients with shortest survival (Fig. 3a, blot 1–5) but not the NG2 low patients with longer survival outcomes (Fig. 3a, blot 6–11). This spot corresponded to the antioxidant enzyme PRDX-1. The mass spectrum of tryptic peptides from the protein spot (22.3 kDa; p*I* 8.27) on Maldi ToF MS is shown in Fig. 3b. MS/MS fragment spectra (post source decay) of the precursors *m/z* 1,211.7 QITVNDLPVGR (Fig. 3b, left and insert) and *m/z* 1,795.0 QGGLGPMNIPLVSDPKR (Fig. 3b, right and insert). The peptide fragments were consistent with in silico fragmentation of QITVNDLPVGR and QGGLG PMNIPLVSDPKR and were both unique for PRDX-1. We confirmed by immunoblotting that the PRDX-1 levels were upregulated in the patient GBMs with the shortest (Fig. 3c, left) compared to those with longer survival outcomes (Fig. 3c, right). In order to functionally test the antioxidant activity of PRDX-1 in the high NG2 expressing GBMs, we measured the end products of lipid peroxidation and found that patient biopsies with high PRDX-1 levels had significantly lower levels of malondialdehyde (MDA) (*T* test, $n = 23$, $p = 0.038$; Fig. 3d). However, PRDX-1 expression was not of prognostic relevance for GBM patient survival ($p > 0.05$, Online Supplementary Figure ESM 1c).

Table 4 Expression of NG2 Nestin and CD133 on tumour cells in patient GBM biopsies

Flow cytometric analysis of NG2, nestin, vimentin and CD133 + (positive), or − (negative) fractions in acutely dissociated GBM biopsies from newly diagnosed and untreated patients

ID	(%) NG2+ Nestin+	(%) NG2+ Nestin+ Vimentin+	(%) NG2+ Nestin+ CD133+	(%) NG2+ Nestin+ CD133−	(%) CD31− CD45− CD133+
2,010-042	62.2	97.6	0.1	99.9	0
2,010-044	43.4	83.2	0	100	0.1
2,010-046	90.7	98.6	1.2	98.8	0.3
2,010-047	34.9	98.8	0.5	99.5	0.1
2,010-048	57.8	87.7	1.9	98.1	0
2,010-062	24.2	96.1	0	100	0
2,010-067	38.2	99.3	8.6	91.4	0.8

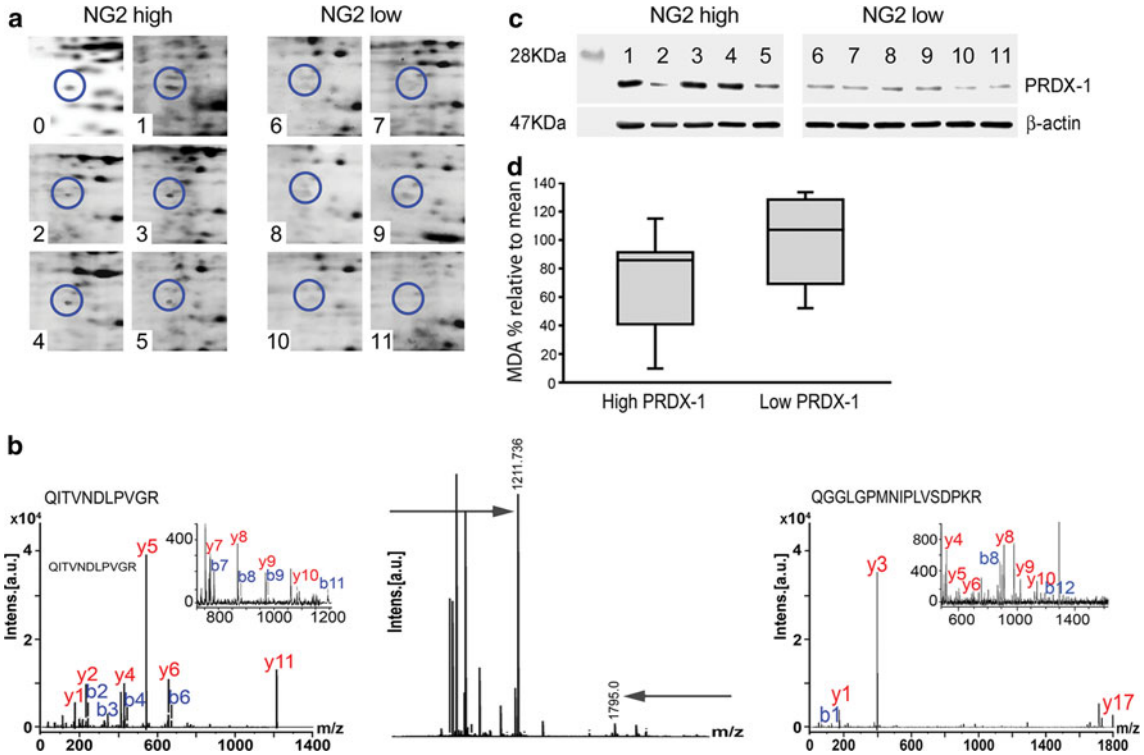

Fig. 3 High PRDX-1 expression in patients with short survival outcomes associate with low lipid peroxidation. **a** 2D gel images of PRDX-1 from 11 patients' GBM biopsies with high (blots *1–5*) and low (blots *6–11*) NG2 expression. Tumour numbers correspond to GBM patient biopsies, except for number 0, which is a master gel of all spots composed by PDQuest. **b** A Maldi TOF/MS of a tryptic digest of the protein spot identifying PRDX-1 (*middle panel*) and MS/MS spectra of two tryptic peptides (*arrows*) corresponding to PRDX-1 with a Mowse score of 198, where <56 was significant at $p = 0.05$, and sequence coverage of 60% (*right and left panels*). Inserts are zoomed regions of the MS/MS spectra of the peptides QITVNDLPVGR and QGGLGPMNIPLVSDPKR, where the *y* ions (*red*) and *b* ions (*blue*) are separated based on their mass to charge ratio (*m/z*) and the peak height represents the relative intensity of the ion peak. **c** Immunoblotting with anti-PRDX-1 antibodies in patient GBM biopsies used in the 2D gels shown. **d** MDA production (nmol/mg protein) in low versus high PRDX-1 expressing GBM biopsies. The data represent %MDA levels relative to the population mean. Data represent SEM, $n = 23$

NG2 expressing cells are more resistant to IR and preferentially induce DNA damage response by efficient activation of G1 and G2 checkpoint

Since both PRDX-1 and NG2 were upregulated in GBM biopsies from the shortest surviving GBM patients with low oxidative damage, we hypothesised that PRDX-1 might protect against ROS-induced damage in the NG2 positive tumours. In order to investigate the role of NG2 and PRDX-1 in oxidative stress, we asked whether shRNA mediated PRDX-1 knockdown (Fig. 4a), could influence the response of NG2 expressing tumours to ionizing radiation. The U251-NG2 cells were significantly more resistant to 5 Gy IR (Two-way ANOVA, $p = 0.001$) compared to the NG2 negative U251 cells. PRDX-1 knockdown significantly sensitised the U251-NG2 cells to both 2 and 5 Gy IR (Two-

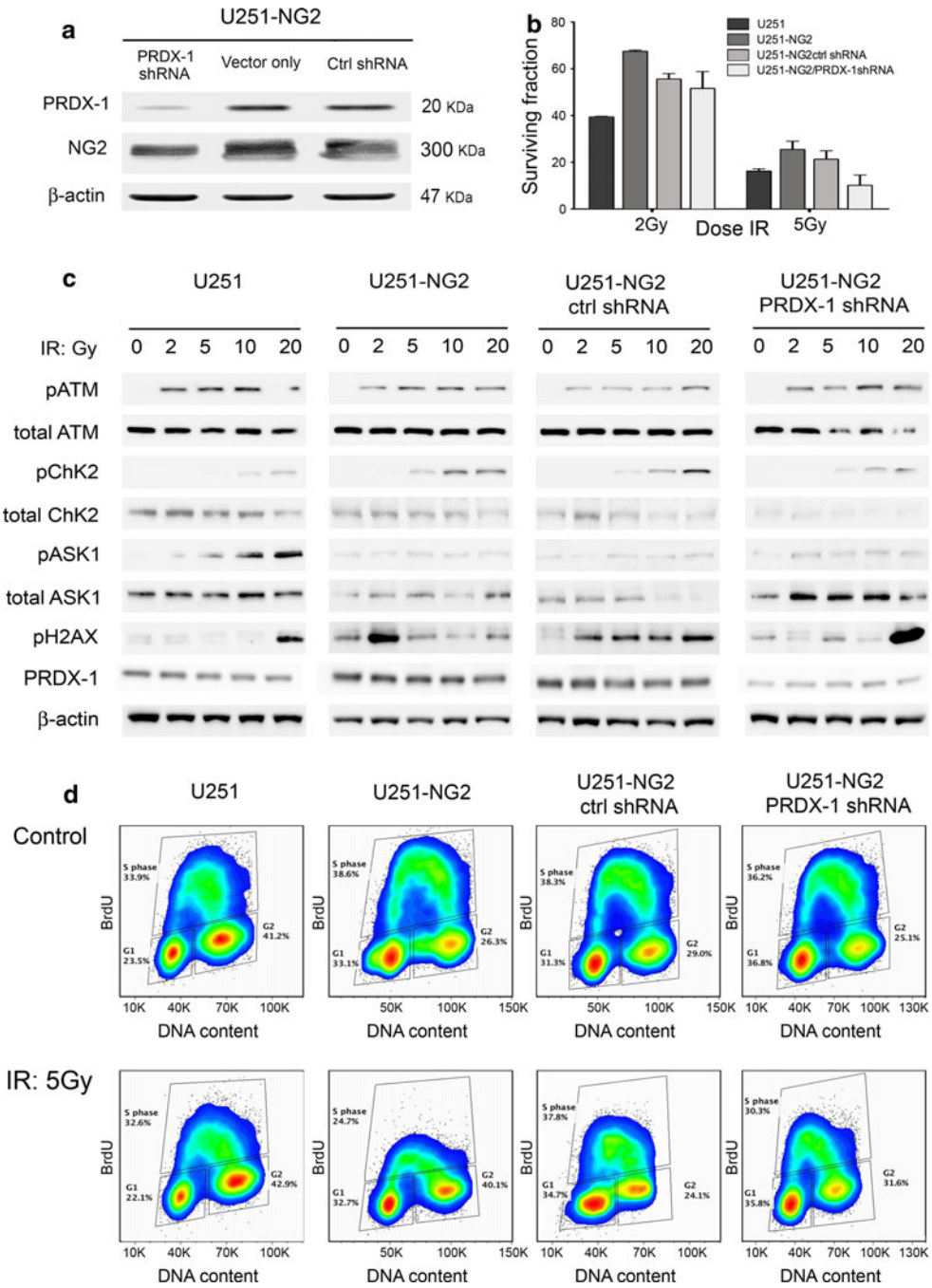

Fig. 4 NG2 positive cells are more resistant to IR and activate checkpoint. **a** Immunoblotting of NG2 expression and stable PRDX-1 protein knockdown, β-actin as control for equal loading. **b** Clonogenic survival 11 days post-treatment with 5 Gy IR. The data represent the mean ± SEM from three independent experiments. **c** Composite immunoblot of phosphorylated ATM, Chk2, (H2AX and ASK1 from multiple blots, 15 min post IR treatment. **d** Bivariate flow cytometric analysis of BrdU uptake and cell cycle distribution determines G1 checkpoint efficiency 2 h post 5 Gy irradiation

way ANOVA, $p = 0.05$, Fig. 4b). Interestingly, the U251-NG2 cells had an increased recognition of IR induced DNA double-strand breaks (DSBs), as indicated by phosphorylated Histone 2A (H2AX), compared to U251 and U251-NG2 shRNA/PRDX-1 cells. U251-NG2 cells showed a marked activation of the checkpoint proteins, pATM and pChk2 compared to U251 and U251-NG2 shRNAPRDX-1 cells (Fig. 4c). Even low dose IR-induced DNA damage immediately activated cell cycle checkpoints as indicated by phosphorylation of γH2AX, ATM and Chk2 proteins in U251-NG2 positive cells (Fig. 4c). In particular, Chk2 was activated in a dose-dependent manner. In contrast, phosphorylation of checkpoint proteins was only evident after high IR doses of 10–20 Gy in the U251 and U251-NG2 shRNA/PRDX-1 cells (Fig. 4c). PRDX-1 levels were consistently higher in the U251-NG2 and U251-NG2 shRNA CTRL cells. PRDX-1 levels were attenuated in the U251 and U251-NG2 shRNA/PRDX-1 cells (Fig. 4c). These findings from these cells with a similar genetic background were confirmed in HF66 cells with endogenous NG2

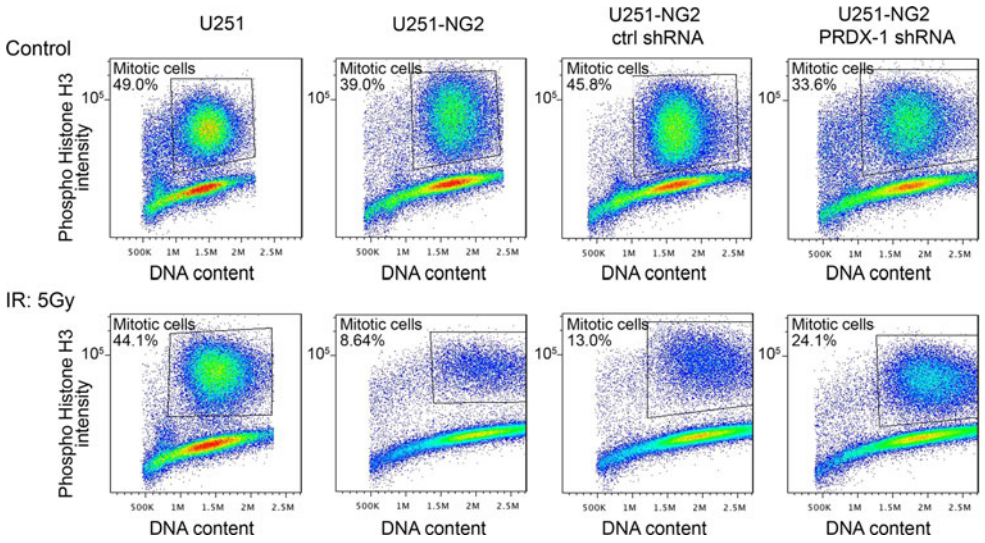

Fig. 5 NG2 positive GBM cells activate G2 checkpoint post irradiation, and this effect is partly abrogated by PRDX-1 knockdown. Activation of G2 checkpoint post 5 Gy irradiation was assessed by flow cytometry. *Plots* display phospho-Histone H3 staining intensity versus DNA Content/cell from one representative of three independent experiments. The percentages of mitotic cells indicate an efficient G2 arrest in the U251-NG2 positive cells and the U251-NG2control shRNA cells (*middle panels*), as fewer cells enter mitosis post irradiation compared to the U251 (*left panels*). Knockdown of PRDX-1 partially abrogates the effect of NG2 on G2 cell cycle checkpoint activity by allowing transition to M-phase post-irradiation (*right panels*)

expression. NG2 knockdown by shRNA (supplementary Figure ESM 2a) sensitised these cells to IR (Supplementary Figure ESM 2b). PRDX-1 and Chk2 were activated in a dose-dependent manner after 2 and 5 Gy in the HF66 wt and HF66 ctrl shRNA cells, which subsequently exited checkpoint, while HF66 NG2 shRNA failed to show dose-dependent PRDX-1 and Chk2 induction (Supplementary Figure ESM 2c).

NG2 mediates G2 checkpoint activation in response to radiation

The induction of DNA damage signalling and activation of cell-cycle checkpoints can be investigated by quantification of BrdU uptake and analysing cell cycle distribution [26]. Quantification of BrdU uptake revealed a prominent G1 checkpoint of the U251-NG2 cells compared to the U251 and U251-NG2 shRNAPRDX-1 cells, as indicated by the reduced number of cells progressing to S-phase (Fig. 4d). In addition, there were greater numbers of U251-NG2 cells arrested in G2 phase of the cell cycle following irradiation (Figs. 4d, 5). Quantification of 4N cells with phosphorylated Histone H3 revealed that mitotic U251-NG2 and U251-NG2 ctrl shRNA cells were diminished after IR compared to the U251 cells, indicating a more efficient G2 checkpoint in the NG2 positive population. Interestingly, the activation of the G2 checkpoint in the NG2 positive cells was abrogated by PRDX-1 shRNA knockdown, demonstrating PRDX-1 as a partial mediator of NG2's effect on G2 checkpoint activation and radiation response (Fig. 5). Despite the rapid DNA damage signalling, the high NG2 expressing cells showed significantly higher survival than U251 and U251-NG2 shPRDX-1 cells 11 days post-irradiation (Fig. 4b). Taken together, our data suggest a role for NG2 and PRDX-1 in mediating radiation resistance through efficient detection of DNA DSBs, and prominent induction of cell-cycle checkpoints.

To determine whether augmented PRDX-1 induction and checkpoint signalling was an NG2 specific response, we knocked down PRDX-1 in the parental U251 cells that do not express NG2 (Supplementary Figure ESM 3a). There was no significant difference in radiation responses in U251 wt, U251 ctrl shRNA or U251-PRDX-1 shRNA-treated cells (Supplementary Figure ESM 3b, Two-way ANOVA, $p = 0.6$). Although PRDX-1 was expressed in parental U251 wt and U251 ctrl shRNA cells but not in U251-PRDX-1 shRNAs after IR, there were no differential responses in the DNA damage and checkpoint signalling in these cells (Supplementary Figure ESM 3c). However compared to NG2 expressing U251-NG2 cells (Fig. 4), these controls exhibited attenuated H2AX and Chk2 activation after IR (Supplementary Figure ESM 3c). Correspondingly, the G1 checkpoint arrest in these control cells after 5 Gy IR was markedly smaller (Supplementary Figure ESM 3d) compared to U251-NG2 cells, and likewise, diminished G2 checkpoint activation (Supplementary Figure ESM 4). These findings indicate a causal link for NG2 in PRDX-1 induction and augmented DNA damage signalling leading to radiation resistance.

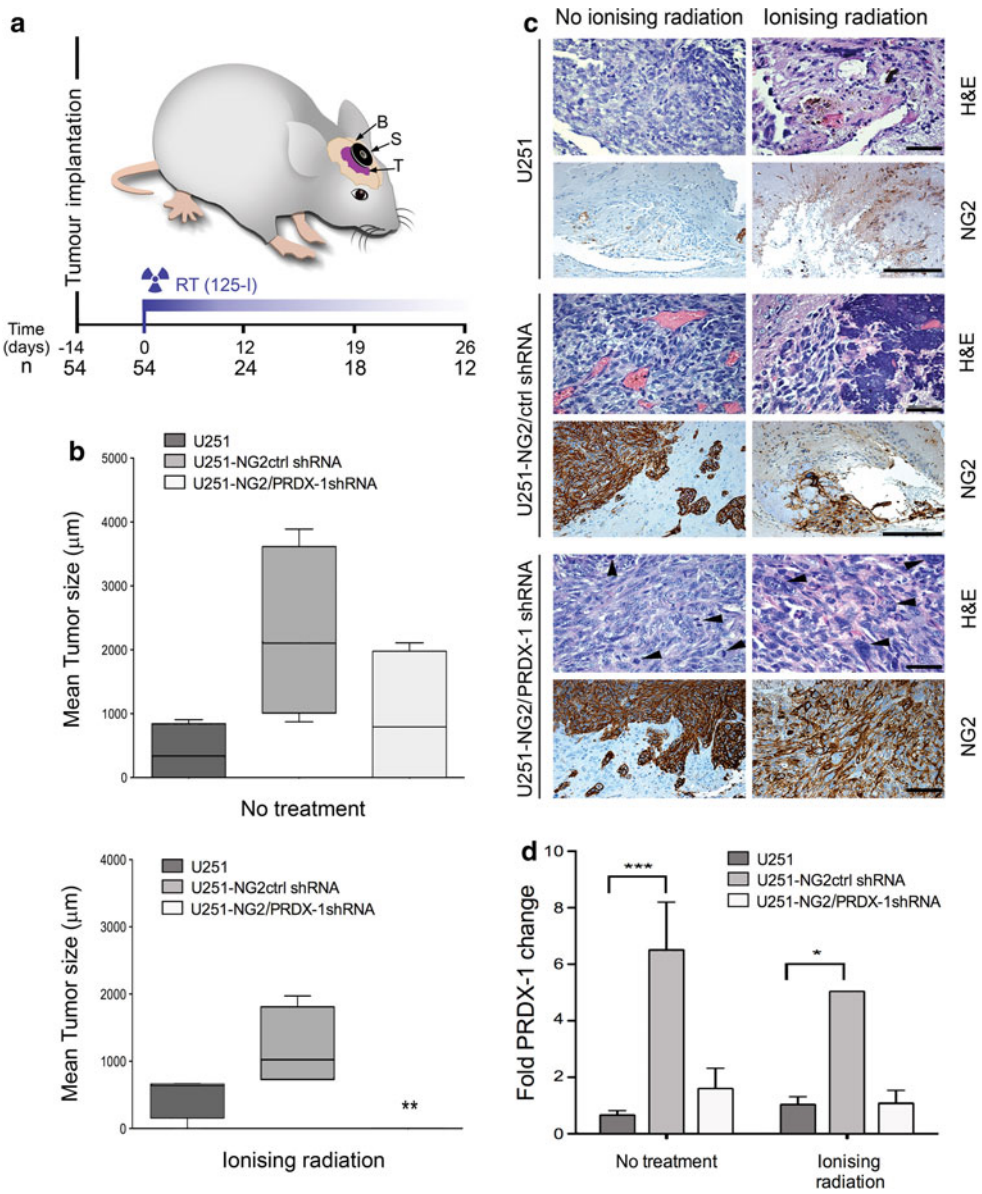

Fig. 6 PRDX-1 knockdown sensitises IR resistant NG2 positive cells in vivo. **a** Schematic of an intracerebral tumour-bearing mouse implanted with ^{125}I seeds. A gradient IR dose (*fading line*) was delivered to the tumour bed. *B* brain, *S* guide-screw, *T* tumour, *n* number of animals (adapted from [50]). **b** Tumour sizes in vivo before IR treatment (*top panel*) and after treatment with ^{125}I (*bottom panel*). **c** Histological staining at 19 weeks with H&E and anti-NG2 antibodies. Note the vascular lakes in the U251-NG2 control shRNA and numerous mitotic figures (*arrowheads*) in U251-NG2/PRDX-1 shRNA tumours, giant multinucleated cells (*arrowheads*). *Scale bars* in all (100 µm; magnification 400×), except rows stained for NG2 (200 µm; magnification 200×). **d** Densitometric quantified, Fold PRDX-1 change in tumour compared to normal brain tissue of mice receiving no treatment or ionizing radiation

To investigate the mechanisms by which PRDX-1 might confer radioprotection, we examined activated apoptosis signalling kinase (ASK1) levels following IR. ASK1 is kept inactive by intramolecular complex with thioredoxins, and ROS oxidise thioredoxin and release it from ASK1. Phosphorylation of ASK1 is cognate for cell death by apoptosis [20]. Phospho-ASK1 levels were elevated in the radiosensitive U251 and U251-PRDX-1 shRNA cells in a radiation dose-dependent manner, whereas phospho-ASK1 levels were unaltered in the radioresistant U251-NG2 cells (Fig. 4c), suggesting that the radioprotective effect of PRDX-1 is mediated by blocking phosphorylation of ASK1.

Suppression of PRDX-1 expression abrogates radiation resistance in vitro but is not sufficient for sustained tumour growth inhibition in vivo

To test whether NG2 expressing cells were also resistant to radiation in vivo, we employed a unique model for concurrent intracranial IR using ^{125}I seeds implanted intracranially in mice (Fig. 6a). The ^{125}I seeds delivered a dose of 1.8 Gy Bio Equivalent $Dose_{tumour}$ (BED_{tumour}) for 12 days at 2.5 mm below the seed, 2.7 Gy in 19 days and 3.5 Gy in 26 days. Untreated U251-NG2 ctrl shRNA tumours reached tumour sizes over 3 mm 12 days post-implantation (Fig. 6b) and were highly vascular and

invaded the brain parenchyma through perivascular infiltration (Fig. 6c). Nevertheless, this invasive phenotype in the xenografts was distinct from that of patient GBMs that display more diffuse invasion of the neuropil by single tumour cells. U251-NG2 tumours expressed sixfold more PRDX-1 protein than U251 tumours in vivo (Fig. 6d). PRDX-1 knock down delayed the growth of U251-NG2 PRDX-1 shRNA tumours compared to U251-NG2 ctrl shRNA and U251 tumours (Fig. 6b) there were no significant difference in tumour-sizes of the different groups (Two-way ANOVA, $p < 0.08$; Fig. 6b). PRDX-1 knockdown partially sensitised U251-NG2 PRDX-1 shRNA cells to IR (Two-way ANOVA, $p < 0.05$; Fig. 6b), while the U251 tumours were entirely growth suppressed and there was no viable tumour evident after 26 days (Two-way ANOVA; $F_{4.420}$; $p < 0.05$). Only haemorrhage and reactive gliosis was evident in remnant lesions from these animals (Fig. 6c). Immunoblotting of the brain lysates revealed that PRDX-1 was indeed stably downregulated in vivo and that the levels were similar to those of the NG2 negative tumours (Fig. 6d), supporting the sensitised response to IR in these animals. The radioresistant U251-NG2ctrl shRNA cells had the greatest PRDX-1 levels both before and after IR (Fig. 6d). Our data collectively establish a role for NG2 as a predictive factor for radiation response in vivo, partially mediated by increased PRDX-1 expression.

Discussion

The present study demonstrates that increased expression of the progenitor marker NG2 on tumour cells and vasculature in GBM biopsies was associated with shorter patient survival, independent of age, clinical treatment and *MGMT* promoter hypermethylation status. NG2 was highly expressed on the surface of tumour cells, including the most pleomorphic cells. However, both NG2 positive and negative tumours exhibited gross chromosomal aberrations that are typical for GBM. Approximately 19% of the GBM cases highly expressed NG2 only on the tumour vasculature, and predominantly on the glomerular-like microvascular proliferations. We have previously demonstrated that overexpression of NG2 in NG2 negative tumour cells produced highly angiogenic tumours characterised by highly tortuous and leaky vasculature [5, 9]. We further demonstrated recently that perturbation of NG2 function with shRNAs abrogated angiogenesis and normalised the tumour vasculature both structurally and functionally in patient GBM-based xenografts [51], indicating a causal role for NG2 in the formation of abnormal tumour vessels. Florid microvascular proliferations are poorly perfused and leaky, due to frequent thrombosis, lack of patent lumen and reduced blood brain barrier integrity. As a consequence, they are commonly located in the vicinity of necrosis where they are thought to contribute to the genesis of the ischemia [24]. Hypoxia promoting microvascular proliferations contribute to radioresistance by reducing the oxygen enhancement effect of IR, inducing gene expression for cell cycle delay and stress proteins, and/or by increased genetic and cellular heterogeneity [19]. The association of high NG2 expression on microvascular proliferations with 60% increased risk of patient mortality and the implications for radioresistance are limited by the retrospective neuropathological nature of the analysis that does not establish causality. We thus investigated the effect of IR in the angiogenic, NG2 expressing tumours in vivo, enabling us to mitigate these retrospective limitations. We were intrigued to note that the NG2 expressing tumours were still more resistant to IR compared to the less angiogenic, U251 tumours, that were completely eliminated in vivo. These findings implicate NG2 as an important factor predicting response to IR rather than differential hypoxic tumour microenvironments. The proportion of cycling U251-NG2 cells was reduced immediately post irradiation, and concomitantly, checkpoint point and DNA damage sensor proteins were activated. Subsequently, a larger fraction of the NG2 positive cells survived irradiation in vitro and in vivo. Collectively, these findings suggest that due to their high metabolic rates, these cells may have evolved a mechanism for surviving DNA damage based on rapid damage detection and checkpoint activation, facilitating repair or availability of survival factors.

The majority of the tumours highly expressed NG2 on both tumour cells and angiogenic vasculature, which is consistent with the high concordance of poor survival outcomes based on tumour or vascular NG2 expression, indicating that multiple mechanisms impacted on the patients' survival outcomes. Indeed, high NG2 expression on both tumour cells and microvascular proliferations increased the risk of death by 155%. These findings have significant clinical implications as NG2 identifies 50% of GBM patients who respond poorly despite optimal treatment. In addition, our data demonstrate that high NG2 expression may override the impact of otherwise favourable prognostic factors such as young age and *MGMT* hypermethylation status. Stratification for age and *MGMT* promoter methylation is mandatory in EORTC clinical trials for GBM, thus we suggest that NG2 may be an additional eligibility factor for identifying the potentially poor responders.

NG2 is an established marker for progenitor cells in various tissues [3], and we have previously shown that it was greatly expressed in GBMs and oligodendrogliomas compared to low-grade tumours [8, 11]. So far it had not been established whether the NG2 positive tumour cells in GBMs represent an immature phenotype. We demonstrated

herein that the vast majority of NG2+ tumour cells co-expressed nestin and vimentin, and that this subpopulation rarely expressed CD133, indicating a possible mesenchymal differentiation phenotype [13]. These findings are supported by cDNA microarray data of the GBM molecular class datasets [37], where searches revealed that the greatest intensity of NG2 gene (*cspg4*) expression was in the GBM with necrosis where 13/50 (26%) exhibited intensity values equal to or greater than 500 [37]. They all fell under the proliferative/mesenchymal subclass with a predominance of genes related to proliferation, wound healing and angiogenesis. This subclass was demonstrated to be associated with poor patient survival [7, 37]. Indeed only 1/6 of the GBMs belonging to the proneural classification (GBM without necrosis) had *cspg4* intensity greater than 500. So, the association of NG2 with poor survival is partially validated by independent datasets and adds to the link between immature cells and GBM aggressiveness [1, 37]. On the other hand, a body of evidence is emerging demonstrating that GBM cells expressing various differentiation markers, irrespective of the stem cell phenotype, may as readily contribute to the aggressive growth of this disease [13, 38]. Loss of heterozygosity of chromosome 10 and gain of chromosome 7 have been linked to the mesenchymal GBM phenotype. Although limited, our array CGH data showed a possible trend in favour of greater frequency or amplitude of relative copy number changes on chromosomes 7 and 10 in the high NG2 expressing tumours. Combined with the flow cytometric data demonstrating high vimentin expression in this subpopulation, this trend is in keeping with the finding of high NG2 expression among the previously reported poor prognosis proliferative and mesenchymal tumour subtypes [37]. It is thus also possible that the prognostic value of NG2 might be partially based on its ability to distinguish molecular tumour subtypes. Further work is required to explore these initial observations. Our data emphasise the complexity of this cancer and the need for individualised therapy based on the tumours genetic and phenotypic composition. We hypothesise that NG2 could be an attractive target in tailored GBM treatment because it is expressed on both the sprouting tumour vasculature and treatment resistant tumour cells.

Upregulation of peroxiredoxin antioxidants has been reported in various solid tumours [23, 32, 35], and is proposed to protect cancer cells from oxidative damage, induced by excessive metabolic activity and anti-cancer treatments. PRDX-1 belongs to the same gene family as PRDX-II, whose expression was induced by IR and chemotherapy [14, 36, 48]. We previously demonstrated that highly aggressive NG2 expressing cell lines and patient GBM spheroids were more resistant to chemotherapy mediated by increased integrin/PI3K/AKT survival signalling [10]. Since these GBM patients also expressed high levels of PRDX-1, our study supports a role for augmented survival signalling that rescues the tumours from lethal DNA damage. Antioxidants inhibit the formation of peroxy radicals and interfere with the subsequent formation of cyclic endo-peroxides to malondialdehyde [39]. Our finding of low MDA levels in high PRDX-1 expressing tumours is consistent with this. Previous work demonstrated that shRNA knockdown of PRDX-II sensitised tumour cells to radiation in vitro due to decreased glutathione reductase activity [46]. Unlike the previous studies examining effects of PRDX-1 depletion on IR response in ectopic tumours [12, 52], we observed only moderate sensitisation to IR by PRDX-1 knockdown in our orthotopic irradiation model. PRDX family members with high functional homology, such as PRDX-II may contribute to scavenge surplus peroxides in the absence of PRDX-1. Moreover, other cell types, such as macrophages are known to produce peroxiredoxins [15]. Thus an alternative approach might have been to knockdown PRDX-1 directly in vivo in all the cell types expressing it. Nevertheless, our patient data extend previous proteomic studies that demonstrated that PRDX-1 was more abundantly expressed in GBMs compared to low grade gliomas [33], and that it predicts the recurrence and shorter survival in stage I non-small cell lung cancer (NSCLC) patients [21]. These findings support a role for PRDX-1 in cancer progression, although its role in GBM radiation response in vivo requires further investigation since we found no association between PRDX-1 expression and patient survival outcomes. Furthermore, analysis of peroxiredoxin gene expression plots on REMBRANDT database revealed no obvious correlation with glioma grade of malignancy since both non-tumour samples as well as various histological types expressed it. Taken together, these findings might be due to functional redundancy in the large PRDX-1 family of antioxidants.

Since stem/progenitor cells can survive cycling hypoxic conditions that produce high levels of ROS (for example the NG2 positive cells), cancer cells that share some of their features may equally survive these hostile conditions by upregulating ROS scavengers such as PRDX-1 [22]. We propose therefore a model (Supplementary Figure ESM 5) where ROS dissociates thioredoxin (PRDX-1) from ASK1, and the latter is phosphorylated and mediates apoptosis via downstream targets such as *c-jun* and P38 MAPKK [20]. In NG2 expressing tumours capable of producing excess PRDX-1, the latter will be readily complexed with ASK1 preventing its activation and subsequent apoptosis. Instead, NG2 expressing cells rapidly activate DNA checkpoints, and survive DNA damage by upregulating the survival factors such as PRDX-1 and PI3K/Akt [10].

In conclusion, high NG2 expression is an important prognostic factor for GBM patient survival independent of age at diagnosis, clinical treatment and *MGMT* promoter

hypermethylation. Multiple mechanisms may be involved, including radiation resistance, partially through mechanisms involving the antioxidant defence systems as well as molecular aberrations at the genetic level. NG2 may be an amenable therapeutic target worth exploring for GBM patients.

Acknowledgments We are grateful to the patients that consented to the use of their biopsy tissue for this research. This work was supported by The Norwegian Cancer Society (PK01-2008-0093), The Meltzer Fond, The Norwegian research Council FRIFORSK, The Bergen Medical Research Foundation, The National Genome Research Network NGFN, Brain Tumour Net (grant 01GS08187, SP8), The German Ministry for Education and Research BMBF. We thank Professor Anders Molven for STR analyses, Professor WB Stallcup and Dr L.J. Stalpers for their generosity with reagents and constructs. We thank Dr Niclou (Norlux laboratory, CRP Sante, Luxembourg) for providing us NCH421k cells used as positive controls for CD133 expression (courtesy of Dr Herold-Mende, Dept Neurosurgery, University of Heidelberg). We are very grateful to Bodil B. Hansen, Tove Johannsen, Solrun Steine, Christine Eriksen, Ingrid Strand for technical assistance and Arwed Weigel at the Molecular Imaging Center (MIC) for assistance with confocal microscopy. Proteomic and cell cycle flow cytometric analyses were performed at PROBE and MIC, respectively, University of Bergen, supported by the National Program for Research in Functional Genomics (FUGE), funded by the Norwegian Research council. Flow cytometric GBM stem cell phenotyping was conducted at Centre de Recherche de Public de la Santé, Luxembourg.

Conflict of interest The authors declare no conflict of interest.

References

1. Bao S, Wu Q, McLendon RE et al (2006) Glioma stem cells promote radioresistance by preferential activation of the DNA damage response. Nature 444:756–760
2. Behm FG, Smith FO, Raimondi SC, Pui CH, Bernstein ID (1996) Human homologue of the rat chondroitin sulfate proteoglycan, NG2, detected by monoclonal antibody 7.1, identifies childhood acute lymphoblastic leukemias with t(4;11)(q21;q23) or t(11;19)(q23;p13) and MLL gene rearrangements. Blood 87:1134–1139
3. Belachew S, Chittajallu R, Aguirre AA et al (2003) Postnatal NG2 proteoglycan-expressing progenitor cells are intrinsically multipotent and generate functional neurons. J Cell Biol 161:169–186
4. Benassi MS, Pazzaglia L, Chiechi A et al (2009) NG2 expression predicts the metastasis formation in soft-tissue sarcoma patients. J Orthop Res 27:135–140
5. Brekke C, Lundervold A, Enger PO et al (2006) NG2 expression regulates vascular morphology and function in human brain tumours. Neuroimage 29:965–976
6. Campos B, Wan F, Farhadi M et al (2010) Differentiation therapy exerts antitumor effects on stem-like glioma cells. Clin Cancer Res 16:2715–2728
7. Chang HY, Nuyten DS, Sneddon JB et al (2005) Robustness, scalability, and integration of a wound-response gene expression signature in predicting breast cancer survival. Proc Natl Acad Sci USA 102:3738–3743
8. Chekenya M, Enger PO, Thorsen F et al (2002) The glial precursor proteoglycan, NG2, is expressed on tumour neovasculature by vascular pericytes in human malignant brain tumours. Neuropathol Appl Neurobiol 28:367–380
9. Chekenya M, Hjelstuen M, Enger PO et al (2002) NG2 proteoglycan promotes angiogenesis-dependent tumor growth in CNS by sequestering angiostatin. Faseb J 16:586–588
10. Chekenya M, Krakstad C, Svendsen A et al (2008) The progenitor cell marker NG2/MPG promotes chemoresistance by activation of integrin-dependent PI3K/Akt signaling. Oncogene 27:5182–5194
11. Chekenya M, Rooprai HK, Davies D et al (1999) The NG2 chondroitin sulfate proteoglycan: role in malignant progression of human brain tumours. Int J Dev Neurosci 17:421–435
12. Chen MF, Keng PC, Shau H et al (2006) Inhibition of lung tumor growth and augmentation of radiosensitivity by decreasing peroxiredoxin I expression. Int J Radiat Oncol Biol Phys 64:581–591
13. Chen R, Nishimura MC, Bumbaca SM et al (2010) A hierarchy of self-renewing tumor-initiating cell types in glioblastoma. Cancer Cell 17:362–375
14. Chung YM, Yoo YD, Park JK, Kim YT, Kim HJ (2001) Increased expression of peroxiredoxin II confers resistance to cisplatin. Anticancer Res 21:1129–1133
15. Conway JP, Kinter M (2006) Dual role of peroxiredoxin I in macrophage-derived foam cells. J Biol Chem 281:27991–28001
16. Franken NA, Rodermond HM, Stap J, Haveman J, van Bree C (2006) Clonogenic assay of cells in vitro. Nat Protoc 1:2315–2319
17. Freier K, Joos S, Flechtenmacher C et al (2003) Tissue microarray analysis reveals site-specific prevalence of oncogene amplifications in head and neck squamous cell carcinoma. Cancer Res 63:1179–1182
18. Hegi ME, Diserens AC, Gorlia T et al (2005) MGMT gene silencing and benefit from temozolomide in glioblastoma. N Engl J Med 352:997–1003
19. Hockel M, Schlenger K, Mitze M, Schaffer U, Vaupel P (1996) Hypoxia and radiation response in human tumors. Semin Radiat Oncol 6:3–9
20. Ichijo H, Nishida E, Irie K et al (1997) Induction of apoptosis by ASK1, a mammalian MAPKKK that activates SAPK/JNK and p38 signaling pathways. Science 275:90–94
21. Kim JH, Bogner PN, Ramnath N et al (2007) Elevated peroxiredoxin 1, but not NF-E2-related factor 2, is an independent prognostic factor for disease recurrence and reduced survival in stage I non-small cell lung cancer. Clin Cancer Res 13:3875–3882
22. Kim YJ, Ahn JY, Liang P et al (2007) Human prx1 gene is a target of Nrf2 and is up-regulated by hypoxia/reoxygenation: implication to tumor biology. Cancer Res 67:546–554
23. Kinnula VL, Lehtonen S, Sormunen R et al (2002) Overexpression of peroxiredoxins I, II, III, V, and VI in malignant mesothelioma. J Pathol 196:316–323
24. Kleihues P, Burger PC, Collins VP et al (2000) Glioblastoma. In: Kleihues P, Cavenee WK (eds) World Health Organisation classification of tumours. Pathology and genetics. Tumours of the central nervous system. IARC Press, Lyon, pp 29–39
25. Li Y, Madigan MC, Lai K et al (2003) Human uveal melanoma expresses NG2 immunoreactivity. Br J Ophthalmol 87:629–632
26. Lieberman HB (2004) Cell cycle checkpoint control protocols. Humana Press, New York
27. Louis DN, Ohgaki H, Wiestler OD et al (2007) The 2007 WHO classification of tumours of the central nervous system. Acta Neuropathol 114:97–109
28. Mauvieux L, Delabesse E, Bourquelot P et al (1999) NG2 expression in MLL rearranged acute myeloid leukaemia is restricted to monoblastic cases. Br J Haematol 107:674–676

29. McLendon RFA, Bigner D, Van Meir EG, Brat DJ, Mastrogianakis GM et al (2008) Comprehensive genomic characterization defines human glioblastoma genes and core pathways. Nature 455:1061–1068
30. Mikeska T, Bock C, El-Maarri O et al (2007) Optimization of quantitative MGMT promoter methylation analysis using pyrosequencing and combined bisulfite restriction analysis. J Mol Diagn 9:368–381
31. Nishiyama A, Dahlin KJ, Prince JT, Johnstone SR, Stallcup WB (1991) The primary structure of NG2, a novel membrane-spanning proteoglycan. J Cell Biol 114:359–371
32. Noh DY, Ahn SJ, Lee RA et al (2001) Overexpression of peroxiredoxin in human breast cancer. Anticancer Res 21:2085–2090
33. Odreman F, Vindigni M, Gonzales ML et al (2005) Proteomic studies on low- and high-grade human brain astrocytomas. J Proteome Res 4:698–708
34. Ohgaki H, Kleihues P (2005) Population-based studies on incidence, survival rates, and genetic alterations in astrocytic and oligodendroglial gliomas. J Neuropathol Exp Neurol 64:479–489
35. Park JH, Kim YS, Lee HL et al (2006) Expression of peroxiredoxin and thioredoxin in human lung cancer and paired normal lung. Respirology 11:269–275
36. Park SH, Chung YM, Lee YS et al (2000) Antisense of human peroxiredoxin II enhances radiation-induced cell death. Clin Cancer Res 6:4915–4920
37. Phillips HS, Kharbanda S, Chen R et al (2006) Molecular subclasses of high-grade glioma predict prognosis, delineate a pattern of disease progression, and resemble stages in neurogenesis. Cancer Cell 9:157–173
38. Prestegarden L, Svendsen A, Wang J et al (2010) Glioma cell populations grouped by different cell type markers drive brain tumor growth. Cancer Res 70:4274–4279
39. Requena JR, Fu MX, Ahmed MU et al (1996) Lipoxidation products as biomarkers of oxidative damage to proteins during lipid peroxidation reactions. Nephrol Dial Transplant 11(Suppl 5):48–53
40. Rhee SG, Kang SW, Chang TS, Jeong W, Kim K (2001) Peroxiredoxin, a novel family of peroxidases. IUBMB Life 52:35–41
41. Riley PA (1994) Free radicals in biology: oxidative stress and the effects of ionizing radiation. Int J Radiat Biol 65:27–33
42. Roepstorff P, Fohlman J (1984) Proposal for a common nomenclature for sequence ions in mass spectra of peptides. Biomed Mass Spectrom 11:601
43. Schrappe M, Klier FG, Spiro RC et al (1991) Correlation of chondroitin sulfate proteoglycan expression on proliferating brain capillary endothelial cells with the malignant phenotype of astroglial cells. Cancer Res 51:4986–4993
44. Shoshan Y, Nishiyama A, Chang A et al (1999) Expression of oligodendrocyte progenitor cell antigens by gliomas: implications for the histogenesis of brain tumors. Proc Natl Acad Sci USA 96:10361–10366
45. Smith FO, Rauch C, Williams DE et al (1996) The human homologue of rat NG2, a chondroitin sulfate proteoglycan, is not expressed on the cell surface of normal hematopoietic cells but is expressed by acute myeloid leukemia blasts from poor-prognosis patients with abnormalities of chromosome band 11q23. Blood 87:1123–1133
46. Smith-Pearson PS, Kooshki M, Spitz DR et al (2008) Decreasing peroxiredoxin II expression decreases glutathione, alters cell cycle distribution, and sensitizes glioma cells to ionizing radiation and H(2)O(2). Free Radic Biol Med 45(8):1178–1189
47. Snijders AM, Nowak N, Segraves R et al (2001) Assembly of microarrays for genome-wide measurement of DNA copy number. Nat Genet 29:263–264
48. Spitz DR, Phillips JW, Adams DT et al (1993) Cellular resistance to oxidative stress is accompanied by resistance to cisplatin: the significance of increased catalase activity and total glutathione in hydrogen peroxide-resistant fibroblasts. J Cell Physiol 156:72–79
49. Stupp R, Mason WP, van den Bent MJ et al (2005) Radiotherapy plus concomitant and adjuvant temozolomide for glioblastoma. N Engl J Med 352:987–996
50. Verhoeff JJ, Stalpers LJ, Coumou AW et al (2007) Experimental iodine-125 seed irradiation of intracerebral brain tumors in nude mice. Radiat Oncol 2:38
51. Wang J, Svendsen A, Kmiecik J et al (2011) Targeting the NG2/CSPG4 proteoglycan retards tumour growth and angiogenesis in preclinical models of GBM and melanoma. PLoS One 6(7):e23062
52. Zhang B, Wang Y, Liu K et al (2008) Adenovirus-mediated transfer of siRNA against peroxiredoxin I enhances the radiosensitivity of human intestinal cancer. Biochem Pharmacol 75:660–667